https://rbgeomorfologia.org.br/
ISSN 2236-5664

Revista Brasileira de Geomorfologia

v. 23, nº 2 (2022)

http://dx.doi.org/10.20502/rbg.v23i2.2084

Artigo de Pesquisa

Model-based assessment of shallow landslides susceptibility at a petrochemical site in Brazil

Análise da suscetibilidade a escorregamentos por meio de modelos de base física em área petroquímica no Brasil

Victor Carvalho Cabral[1], Fábio Augusto Gomes Vieira Reis[2], Carolina Martinez Mendoza[3], Alan de Oliveira[4]

[1] Universidade Estadual Paulista - UNESP, Departamento de Geologia Aplicada, Rio Claro, Brasil. E-mail: victor.carvalho@unesp.br
ORCID: https://orcid.org/0000-0002-9910-0508

[2] Universidade Estadual Paulista - UNESP, Departamento de Geologia Aplicada, Rio Claro, Brasil. E-mail: fabio.reis@unesp.br
ORCID: https://orcid.org/ 0000-0003-3918-6861

[3] Universidad del Norte, Departament of Physics and Geosciences, Barranquilla, Colômbia. E-mail: martinezcarolina@uninorte.edu.co
ORCID: https://orcid.org/0000-0002-5861-5062

[4] Universidade Estadual Paulista - UNESP, Departamento de Geologia Aplicada, Rio Claro, Brasil. E-mail: alan.oliveira@unesp.br

Recebido: 20/01/2021; Aceito: 01/06/2021; Publicado: 06/04/2022

Resumo: A região da Serra do Mar é altamente suscetível ao desencadeamento de escorregamentos translacionais rasos devido ao seu clima e relevo. A aplicação de modelos de bases físicas é um método objetivo de caracterizar a suscetibilidade a escorregamentos, sendo de grande importância em estudos e avaliações de perigo e risco. O objetivo desse estudo é a comparação entre cenários de suscetibilidade a escorregamentos utilizando os modelos SHALSTAB e SINMAP em duas bacias hidrográficas (Mogi e Perequê) em Cubatão, maior polo petroquímico da América Latina. A calibração dos modelos é baseada no inventário de cicatrizes de escorregamento do evento de 1985, enquanto que os parâmetros topográficos são baseados no modelo digital de elevação (MDE) e os parâmetros geotécnicos obtidos a partir de amostras de solo. Por meio da análise *Receiver Operating Characteristics* (ROC) na comparação dos modelos, os resultados indicam que o SHALSTAB é o modelo que melhor se aplica à região de estudo em escala regional, uma vez que apresenta maior concentração de cicatrizes em áreas potencialmente instáveis (resultados verdadeiros positivos) e maior acurácia. Embora SINMAP apresente resultados com grau semelhante de sucesso, o modelo é menos acurado e falha com maior frequência na identificação de áreas potencialmente instáveis.

Palavras-chave: Serra do Mar; SINMAP; SHALSTAB.

Abstract : The Serra do Mar mountain range is the main site of shallow-landslides occurrence in Brazil. The application of physically-based models is an effective method to predict landslide susceptibility, which is of great importance in hazard assessments and urban-planning studies. Thus, the objective of this study is to compare landslide susceptibility scenarios created with SHALSTAB and SINMAP at two large watersheds (Mogi and Perequê) in Cubatão, Latin America's largest petrochemical site. Model calibration is based on the landslide scars inventory of the 1985 event, the geotechnical parameters derived from soil samples and the topography sourced from a 5 m resolution DEM. Using the Receiver Operating Characteristics (ROC) analysis to assess model performance, SHALSTAB emerges as the best-fit model for both watersheds due to higher concentration of landslide scars in unstable areas (true positive results) and higher global accuracy. Even though SINMAP had similar degree of success, it was slightly less accurate and failed more often in the identification of potentially

unstable areas. Comparative performance studies of physically-based models are fundamental to support effective and reliable hazard assessments in mountain regions, providing an outlook in how to proceed with more detailed studies.

Keywords : Serra do Mar; SINMAP; SHALSTAB.

1. Introduction

Gravitational mass movements are part of the natural evolution of the landform and can represent great hazard to humans in mountain regions (GUIDICINI e NIEBLE, 1984). While there have been several advances in hazard and susceptibility assessment of mass-movement-prone areas (e.g., GIS tools application), climate change, increasing deforestation and urbanization contribute to the intensification of the frequency and risk of these phenomena (SCHUSTER, 1996; DIETRICH *et al.*, 1998; GOETZ *et al.*, 2011). Among the different mass-movement types, shallow landslides triggered by rainfall are one the most costly and dangerous natural hazards (PETLEY, 2012; KOBYIAMA *et al.*, 2015), and the potential increase in the occurrence of extreme precipitation events due to climate change is of great concern globally (AHERN *et al*., 2005; KNAPP *et al*., 2008; HALLEGATTE *et al*., 2013 WESTRA *et al*., 2014).

The Serra do Mar mountain range, with steep slopes (averaging 30º to 35º) and high rainfall rates, is the main site of shallow landslides events in Brazil (IPT, 1986; TATIZANA *et al.,* 1987). The mountain range extends for about 1,500 km in the Brazilian southern and southeastern coast (VIEIRA; GRAMANI, 2015), with several municipalities and infrastructures located on and at the foot of the hillslopes. Cubatão (State of São Paulo), the largest petrochemical site in Latin America, is an example of a city that developed immediate to Serra do Mar, periodically experiencing losses due to mass-wasting processes. The regional landslide event of February 1994 is a prime example, affecting an oil refinery and causing more than U$40 million in damages (LOPES *et al*., 2007).

One of the greatest challenges in hazard assessment of landslide-prone regions is to predict the initiation area of these phenomena, which can avoid and mitigate social and economic losses (MONTGOMERY; DIETRICH, 1994; PACK *et al*., 1998). Physically-based models were developed to describe shallow landslides susceptibility in mountain regions through the direct application of physical equations, predicting landslide initiation under different geotechnical and climate scenarios (BAUM *et al*., 2002). By coupling hydrological and slope stability models to identify areas that are prone to triggering landslides, these models can provide important insights that can support urban planning and hazard assessment studies (GUZZETTI *et al*., 1999; VAN WESTEN, 2004; BEL *et al*., 2016).

TRIGRS (*Transient Rainfall Infiltration and Grid-Based Regional Slope Stability model*; BAUM *et al*., 2002), SINMAP (*Stability Index Mapping*; PACK *et al*., 1998), and SHALSTAB (*Shallow Landslide Stability model*; MONTGOMERY; DIETRICH, 1994) are the most commonly used models in landslide susceptibility assessments. These models exhibit different complexity levels and their output quality are strongly dependent on the input geotechnical and topographic parameters (ZIZIOLI *et al*., 2013), with most studies applied at slope scale or at <10 km² watersheds, where higher control on data quality is possible (e.g., MORRISSEY *et al*., 2001; RAFAELLI *et al*., 2001; CLAESSENS *et al*., 2005; GODT *et al*., 2008; LIU e WU, 2008; CAPARELLI; VERSACE, 2011; GOETZ *et al*., 2011; NIKOLOPOULOS *et al*., 2015; WU *et al*., 2015; ALVIOLI; BAUM, 2016; GIANNECCHINI *et al*., 2016, THIEBES *et al*., 2016; LIU *et al*., 2016; SIMÕES *et al*., 2016; PRIETO *et al*., 2017; AFFANDANI; KUSRATMOKO, 2019; KÖNIG *et al*., 2019; AVILA *et al*., 2020).

These models have also been successfully applied in slope stability studies at Serra do Mar (e.g., FERNANDES *et al*., 2001; GUIMARÃES *et al*., 2003; GOMES, 2006; GUIMARÃES *et al*., 2009; REGINATO *et al*., 2013; MICHEL *et al*., 2014; NERY e VIEIRA, 2015; SBROGLIA *et al*., 2016; ROSOLEM *et al*., 2017; CARDOZO *et al*., 2018; VIEIRA *et*

al., 2018; CABRAL; REIS, 2020), with SHALSTAB and SINMAP arguably the most commonly used. Both SHALSTAB and SINMAP have similar physical principles (hydrological model combined with a *Mohr-Coulomb*-based infinite-slope model), though SHALSTAB, deterministic, is generally recommended for localized slopes and small watersheds (MONTGOMERY; DIETRICH, 1994; DIETRICH *et al*., 2001) and SINMAP, stochastic, for regional scale studies (PACK *et al*., 1998; LOPES *et al*., 2007).

Even though the application of physically-based models has been extensively covered in the literature, comparative performance studies are less common and few of them focus on large watersheds. Thus, the objective of this study is to compare landslide susceptibility scenarios created using SHALSTAB and SINMAP in the Perequê and Mogi watersheds, two large basins (>30 km²) in Cubatão (State of São Paulo), to identify the most representative of the chosen area. The research contributes to the identification of the factors that influence slope stability at Serra do Mar, as well as to the reliability of future hazard assessment studies using physically-based models.

2. Study area

Figure 1 shows the location of the watersheds Perequê and Mogi. The watersheds have a combined area of 86.9 km², with elevations that range from 10 m to 1,060 m in the larger Mogi (56.8 km²) and 10 m to 900 m in the Perequê (30.1 km²). Mogi and Perequê are within the geomorphological context of the Serra do Mar mountain range, a set of festooned escarpments with one face declining abruptly towards the Atlantic Ocean and the opposite declining gently inland (SELUCHI *et al*., 2010, VIEIRA; GRAMANI, 2015).

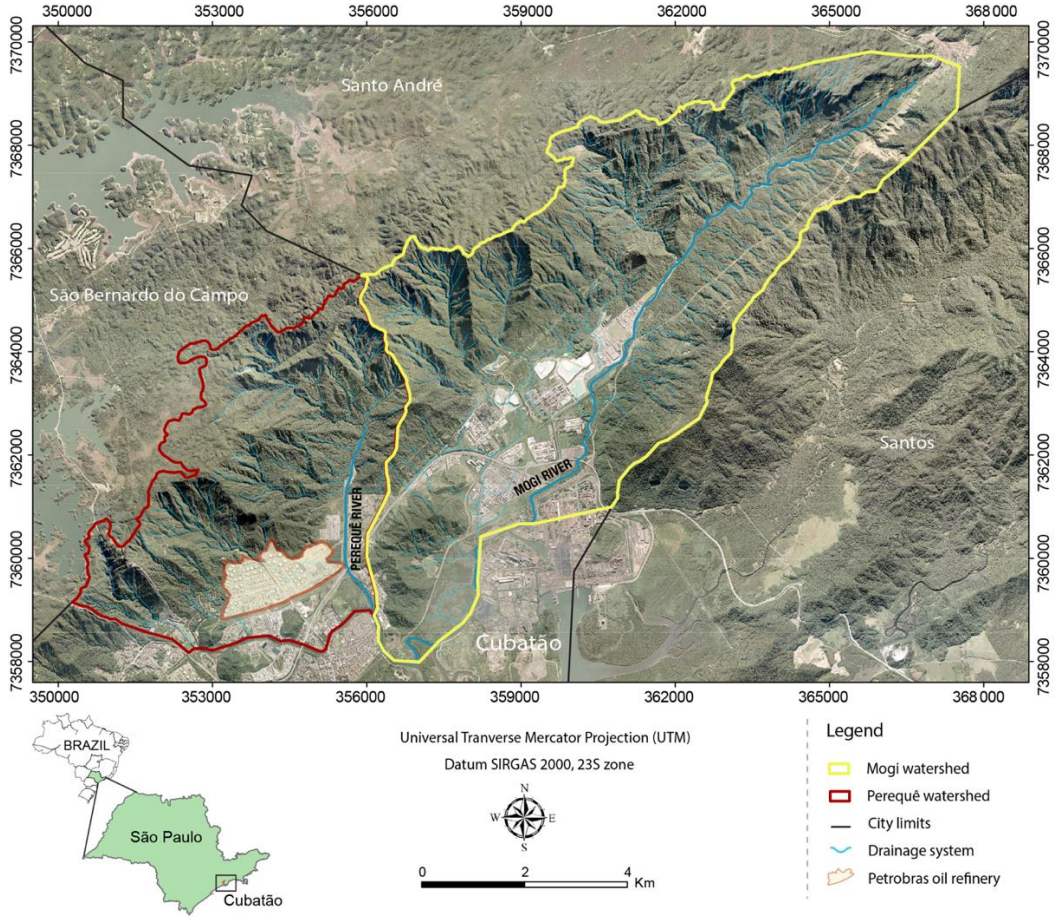

Figure 1. Location of the watersheds Mogi and Perequê in Cubatão, State of São Paulo, Brazil. Orthorectified aerial photograph from 2011, at a 1:400 scale, provided by the Metropolitan Planning Company of the State of São Paulo (EMPLASA).

The watersheds are characterized by mid to high gradients (averaging 65% or 33º) and the geology is mainly comprised of Archean/Proterozoic metamorphic (gneiss) and magmatic (granitoid) rocks, which combined with the physiographic characteristics results in thin (up to 3-4 m deep) residual soil (WOLLE; CARVALHO, 1994; VIEIRA *et al*., 2015). Bedrock also impacts the soil's physical and hydrological properties, controlling the type and frequency of landslides (VAN ASCH *et al*., 1999). Shallow landslides predominate at the study area and the soil generally exhibits a high sand concentration, with cohesion ranging from 0 kPa to 6 kPa and saturated hydraulic conductivity (K_s) from 10^{-6} m s^{-1} to 10^{-4} m s^{-1} (WOLLE; CARVALHO, 1994). Figure 2 shows the 1:50,000 geological map of the study region, adapted from the Institute for Technological Research - IPT (1986).

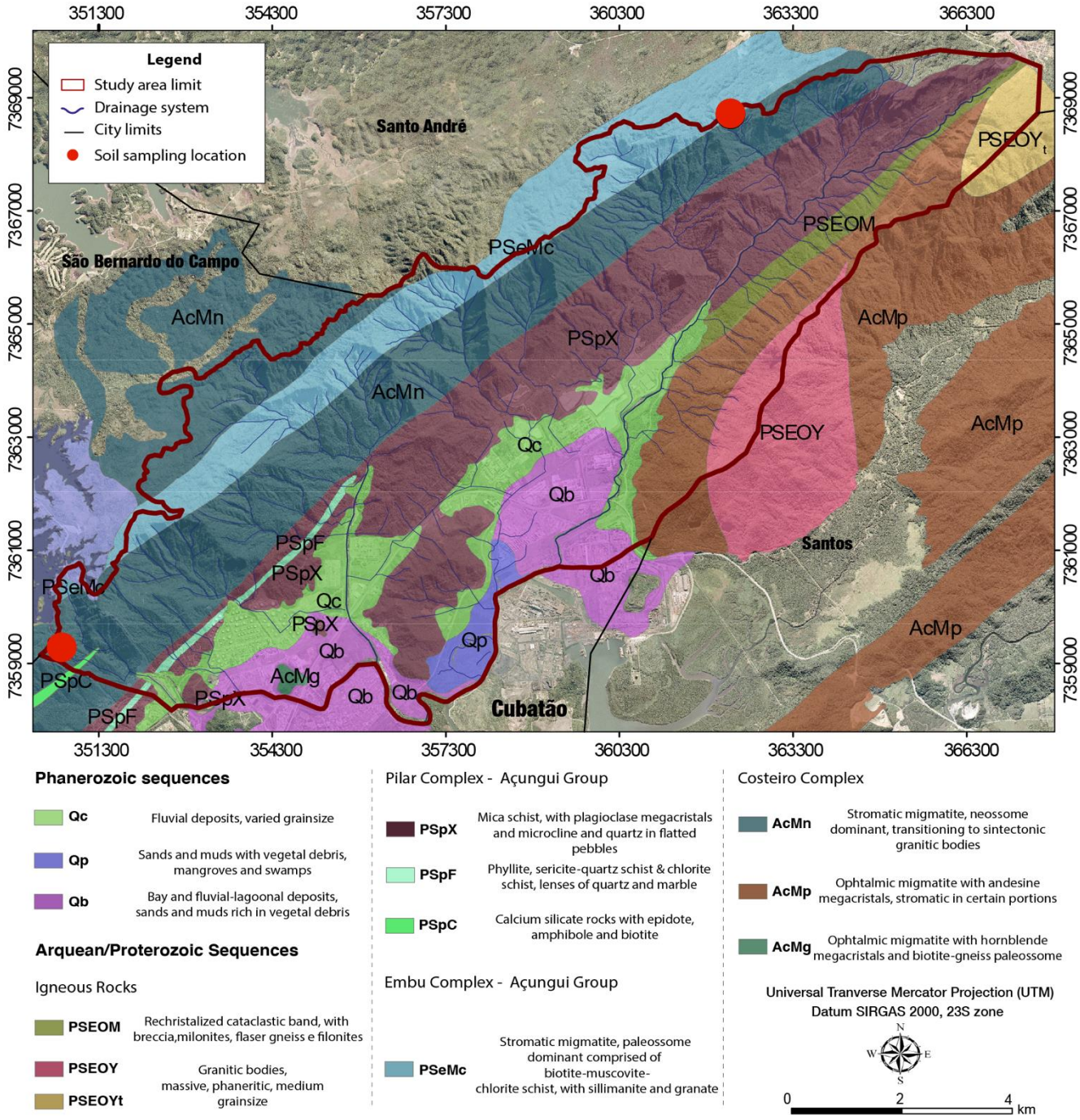

Figure 2. Geological map of the study area, based on the mapping made by the Institute of Technological Research – IPT (1986) at a 1:50,000 scale. Location of soil samples used in this study are obtained from Wolle and Carvalho (1989).

The region is characterized by a subtropical-humid climate (Cfa – Köppen classification), with temperatures that vary from 17º to 36º during the year (LOPES *et al*., 2007). The average annual rainfall index in Cubatão can surpass 3,300 mm, reaching up to more than 4,000 mm in some years (KANJI *et al*., 2007). The South Atlantic Convergence Zone associated with blocking systems over the Atlantic Ocean often creates a situation prone to landslide-triggering in Serra do Mar, with convective rainfall enhanced due to orographic effect the most common landslide-triggering type (VERA *et al*., 2006). Due to heavy and extreme rainfall events, several major catastrophic landslide events have been recorded throughout Cubatão history (MASSAD *et al*., 1997; 2000; WOLLE; CARVALHO, 1989).

In this study, the 1985 regional landslide event is chosen to calibrate and assess modeling results, due to its great proportions and wide spatial distribution across both Perequê and Mogi (Fig. 3). According to rain gauge data from the Water Resource Management System of the Department of Water and Energy of the State of São Paulo (DAEE), the event was triggered by a 265 mm rainfall in 24-h (between the 23rd and 24th of January), causing an industrial pipe containing ammonia to break in Mogi's sub-catchment 'Copebrás' and, consequently, resulting in great environmental damage (MASSAD *et al*., 2000; LOPES *et al*., 2007; KANJI *et al*., 2007). The production and storage of chemical and highly flammable products within the watersheds' limits (especially in Perequê, where an oil refinery is located) pose considerable financial, social and environmental hazard.

Figure 3. Shallow landslides of the 1985 event in Cubatão. Pictures from IPT (1986).

3. Material and Methods

3.1. The Models

The Factor of Safety (FS) is the most commonly applied method in slope stability analysis, especially in shallow landslide susceptibility studies (WOLLE; CARVALHO, 1994; LIU; WU, 2008). SHALSTAB and SINMAP are based on the coupling of an infinite-slope and a hydrology model to calculate FS, as extensively covered in the literature (e.g., MONTGOMERY; DIETRICH, 1994; PACK *et al*., 1998, among others). The infinite-slope model is based on the *Mohr-Coulomb* Law, which dictates that in the moment of slope failure, shear forces (τ) are superior to shear-resistant forces, such as soil cohesion (c) and internal friction angles (φ), due to Normal Stress (σ) in the rupture surface (Eq. 1). μ is soil's pore-pressure that opposes the Normal.

$$\boldsymbol{\tau = c + (\sigma - \mu) * tan\varphi} \quad (1)$$

The steady-state subsurface flow, described in TOPOMODEL (BEVEN; KIRKBY, 1979) and TOPOG (O'LOUGHLIN, 1986), is the most often used hydrological concept in slope stability modeling. The hydrological model adopts a uniform recharge that simulates the spatial variation of the water table during precipitation, where Wetness (*W*) is given by the ratio between precipitation (*q*) and soil's transmissivity (*T*) (O'LOUGHLIN, 1986). Eq. 2 shows the steady-state hydrological model, where *a* is drained area (m^2), *b* is contour length element (m), θ is mean slope (º, degrees), *h* is water level (m) and *z* is soil depth (m). Eq. 3 shows the transmissivity calculation, where K_s is the saturated hydraulic conductivity (m s^{-1}).

$$\boldsymbol{W = \frac{q * a}{b * T * sin\theta} = \frac{h}{z}} \tag{2}$$

$$\boldsymbol{T = K_s * z * \cos\theta} \tag{3}$$

SINMAP, based on the FS, calculates the probability of a location to be stable, assuming uniform distribution of the input parameters across the study area over an admitted "uncertainty range" (PACK *et al*., 1998). A more detailed description of the model and its governing equations can be found on Pack *et al*. (1998) and the final formulation of SINMAP is shown in Eq. 4:

$$\boldsymbol{FS = \frac{C + \cos\theta \left[1 - \min\left(\frac{q}{T\sin\theta}\right) r, 1\right] \tan\varphi}{\sin\theta}} \tag{4}$$

$$\boldsymbol{C = \frac{C_s + C_r}{z * \rho_s * g}} \tag{5}$$

Where *C* is the dimensionless cohesion, *q* is the effective rainfall (m^2 h^{-1}), *T* is soil transmissivity (m^2 h^{-1}), θ is the slope angle (º, degrees), φ is the internal friction angle of the soil (º, degrees) and *r* is the water to soil density ratio (ρ_w/ρ_s). *C* (Eq. 5) is based on soil cohesion (C_s, N m^{-2}), soil density ($\boldsymbol{\rho}$s, kg m^{-3}) and soil depth (*z*, m), as well as a standard gravity (*g*, m s^{-2}) - assumed in this study as 9.81 m s^{-2}. Root cohesion (C_r) is challenging to estimate and is excluded from calculation (set as 0), as suggested by Montgomery and Dietrich (1994) and Meisina and Scarabelli (2007).

SINMAP classifies the study area according to six different Stability Index (SI) classes: Stable, Moderately Stable, Quasi Stable, Lower Threshold, Upper Threshold and Unconditionally Unstable (Table 1). The first three classes have FS > 1, indicating that these areas should not fail with the most conservative parameters in the specified range (PACK *et al*., 1998). For the Lower and Upper Thresholds, FS is lower than 1 and the probability of failure is, respectively, lower and greater than 50 %. For the last stability class, the probability of failure in the specified range is > 90%.

SHALSTAB assumes that the local topography is the main controlling factor in shallow landslide occurrence and calculates the critical steady-state rainfall needed for triggering slope failures in the landform, based on the ratio of effective rainfall to soil transmissivity (*q*/*T*) (MONTGOMERY; DIETRICH, 1994). A more detailed description of the model and its governing equations is presented in Montgomery and Dietrich (1994), with Eq. 6 showing the final formulation of SHALSTAB:

$$\boldsymbol{\frac{q}{T} = \frac{b}{a} * sin\theta \left\{\left(\frac{\rho_s}{\rho_w}\right) * \left(1 - \frac{tan\theta}{tan\phi}\right) + \left(\frac{c}{\rho_w * g * z * cos^2\theta * tan\phi}\right)\right\}} \tag{6}$$

Where *q* is the critical rainfall required to initiate slope failure (m), *T* is soil Transmissivity (m^2 day^{-1}), *a* is upslope contributing area (m^2), *b* is the contour length (m), *C* is soil cohesion (Pa), θ is slope angle (º, degrees), ρ_w is water density (kN m^{-3}), ρ_s soil density (kN m^{-3}), *g* is gravitational acceleration (m s^{-2}), *z* is soil thickness (m) and φ is internal friction angle of the soil (º, degrees).

SHALSTAB classifies the analyzed area into seven stability classes, as shown in Table 2. Lower Log *q*/*T* values indicate a greater tendency for instability and higher values a greater chance of stability, encompassing also areas

where slope instability should occur even under dry conditions (Chronically unstable) and areas that are stable even under rainfall rates of >1,000 mm day^{-1} (Stable).

Table 1. SINMAP Stability classes, after Pack *et al*. (1998).

Stability Index	Stability Classes	Parameter range	Possible influence of factors not modeled
> 1.5	Stable	Instability range not modelled	Significant destabilizing factors are required for instability
1.5 to 1.25	Quasi-stable	Instability range not modelled	Moderate destabilizing factors are required for instability
1.25 to 1.0	Moderately stable	Instability range not modelled	Minor destabilizing factors could lead to instability
1.0 to 0.5	Lower threshold	Pessimistic half of range necessary for instability	Destabilizing factors are not required for instability
0.5 to 0	Upper threshold	Optimistic half of range necessary for stability	Stabilizing factor may be responsible for instability
< 0	Defended	Range cannot model stability	Stabilizing factors are required for stability

Table 2. SHALSTAB Stability classes, according to Montgomery and Dietrich (1994).

Log intervals (q/T)	Stability classes
Stable	Unconditionally stable and saturated
> -2.2	Unconditionally stable and non-saturated
-2.5 to -2.2	Stable and non-saturated
-2.8 to -2.5	Unstable and non-saturated
-3.1 to -2.8	Unstable and saturated
< -3.1	Unconditionally unstable and non-saturated
Chronically unstable	Unconditionally unstable and saturated

Subsurface hydrologic boundaries parallel to surface, uniform soil thickness and hydraulic conductivity and steady-state subsurface flow are common assumptions used in both SINMAP and SHALSTAB (ZIZIOLI *et al*., 2013).

3.2. Landform and Rainfall Database

The digital elevation model (DEM) is essential in SINMAP and SHALSTAB application, sourcing topographic parameters required for landslide modeling, such as the variables a, b and θ (GUIMARÃES *et al*., 2003). DEM resolution, therefore, must be as representative as possible of the topography, considering the scale of the study and the available data (DIETRICH *et al*., 2001; CLAESSENS *et al*., 2005). A 5 m resolution DEM is adopted, based on a 1:10,000 topographic map provided by the Geographic and Cartographic Institute of the State of São Paulo – IGC (Fig. 4). The DEM was created using the *Topo to Raster* tool of ArcGIS 10.1.

The landslide scars inventory used in performance assessment was based on black and white stereoscopic aerial photographs from April 1985, also provided by IGC at a 1:25,000 scale. 1,679 landslide scars were mapped in the two watersheds (Figure 4), with an average area of ca. 338 m^2. 1,199 out of the 1,679 landslides scars were

mapped in the Mogi watershed, where the landslides exhibit a larger average area (419 m²) compared to Perequê (257 m²). Landslide scars in both watersheds are concentrated in slopes averaging 58% (30º) and at elevations between 600 and 750 m.

The criteria used in landslide scars identification were: lack of vegetation, characteristic morphology (elongated, length superior to width) and drainage conditions of hillslopes (SOETERS; VAN WESTEN, 1996; MOINE *et al*., 2010). Only the upper portion of the scars is considered in the inventory created (Fig. 4), since the chosen models can only predict the initiation areas of the landslides during simulations and not their paths.

The rainfall data of the 1985 landslide event was retrieved from the rainfall database of the Department of Water and Energy of the State of São Paulo (DAEE), based on five pluviometers around the study area (Fig. 4 and Table 3). Between the 23rd and 24th of January, rainfall reached ca. 412 mm in 48-h (more than what is expected for the whole month), with a 24-h accumulated index of 265 mm and peak precipitation of 84 mm h^{-1} (KANJI *et al*., 2007). Even though only one of the pluviometers is located at the top of the hillslopes (i.e., rainfall indexes can be underestimated on those at the valley), the rainfall event was probably concentrated at the central and northeastern part of the Mogi watershed, where there is a higher density of landslide scars (CABRAL *et al*., 2019).

Table 3. Consolidated rainfall indices for the 23rd and 24th of January, 1985, compared to summer months average (1950-2013). Data retrieved from the pluviometer database of the Department of Water and Energy of the State of São Paulo. Avg. = average.

Rain gauge	Name	Elevation (m)	Rainfall indices		
			Summer months avg. (mm)	Jan 23 (mm)	Jan 24 (mm)
E3-038	Piaçaguera	2	325.6	150	110
E3-101	Cubatão	2	317.2	136.2	104.3
E3-144	Morro do Piche	10	302.1	95.1	85.5
E3-149	Campo Grande	780	323.1	241.5	169.8

3.3. Geotechnical Parameters

The input parameters are based on soil samples collected in the study area by the Institute of Technological Research (IPT), presented in Wolle and Carvalho (1994). These samples were collected in colluvial soils and saprolite from migmatite and gneiss-derived regolith (location in Fig. 2). The colluvial samples were collected at 1-3 m depth, with a sandy-clayey texture, and the saprolite samples at a 3 - 4 m depth, with a sandy texture (WOLLE; CARVALHO, 1989). Soil sample density is low when the dimension of the study area is considered, but due to the lack of quantitative information on the physical parameters of the region's soil and the relative homogeneity of the geology (and, consequently, the geotechnical characteristics), these samples are considered representative of the central and eastern hillslopes of Cubatão.

Three different scenarios were considered in simulations: scenario 1 based on the minimum values of the colluvial soil tests, scenario 2 based on the average values and scenario 3 based on the maximum values. Only colluvial samples are considered since, according to our field investigations, the soil involved in shallow landslides are superficial colluvial deposits. Two field campaigns (February and October, 2018) were made at the study area, to confirm the lithological and pedological characteristics of the study area, as well to confirm modelling results and sample the region's soil. Our own samples are not used in this study due to technical issues with sampling transport, which prohibited triaxial shear tests.

Even though tests of cohesion and internal friction angle were not possible, our eight (8) samples corroborate soil density values and texture from Wolle and Carvalho (1994). The samples were collected at a ca. 1 m (Fig. 5a) and 2 m depth in colluvial soils (Fig. 5b) and in areas where landslide scars were present (Fig. 5c and 5d). The

density (ρ_s) values of our soil samples vary from 12 kN m^{-3} and 17.55 kN m^{-3}, with a sandy-clayey texture and porosity that ranges from 46% to 50%. Sampling locations are indicated in Figure 4. Since the study area is located in a State Park ("*Parque Estadual da Serra do Mar*"), minimal disturbance of the soil and vegetation was made and a prior approval from the State's Environmental Department (*Secretaria do Meio Ambiente*) was obtained through the *Instituto Florestal* (Processo SMA no. 260108-005.552/2017).

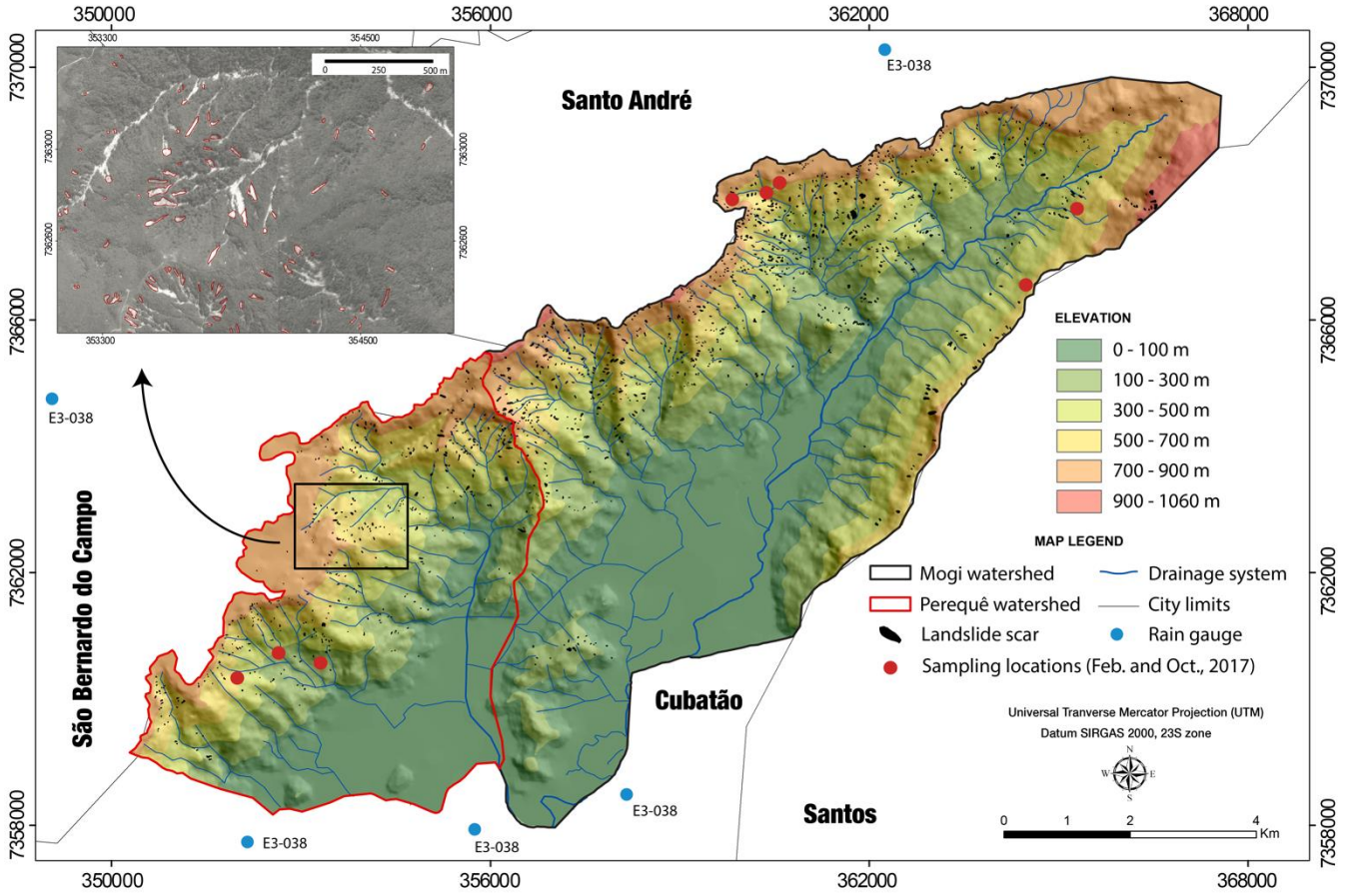

Figure 4. Landslide scars inventory overlayed upon the hypsometric map of the study area. The location of the rain gauges used in this study is also indicated, as well as the sampling locations from our field investigations. In detail, the aerial photographs that sourced the identification of the landslide scars' initiation area.

The input parameters of SHALSTAB and SINMAP are shown, respectively, in table 4 and 5. SINMAP considers climate and hydrogeological factors in its input data, via the T/q parameter (soil transmissivity / effective rainfall). The effective rainfall, defined here as the total precipitation minus evapotranspiration and infiltration (MEISINA; SCARABELLI, 2007), is assumed to be 75% of the total rainfall in 24-h. The saturated hydraulic conductivity (K_s) varies from 10^{-6} m s^{-1} to 10^{-4} m s^{-1} (WOLLE; CARVALHO, 1994). Moreover, differently from SHALSTAB, SINMAP does not indicate absolute values that best represent slope stability, but a range at which the probability of slope failure is higher.

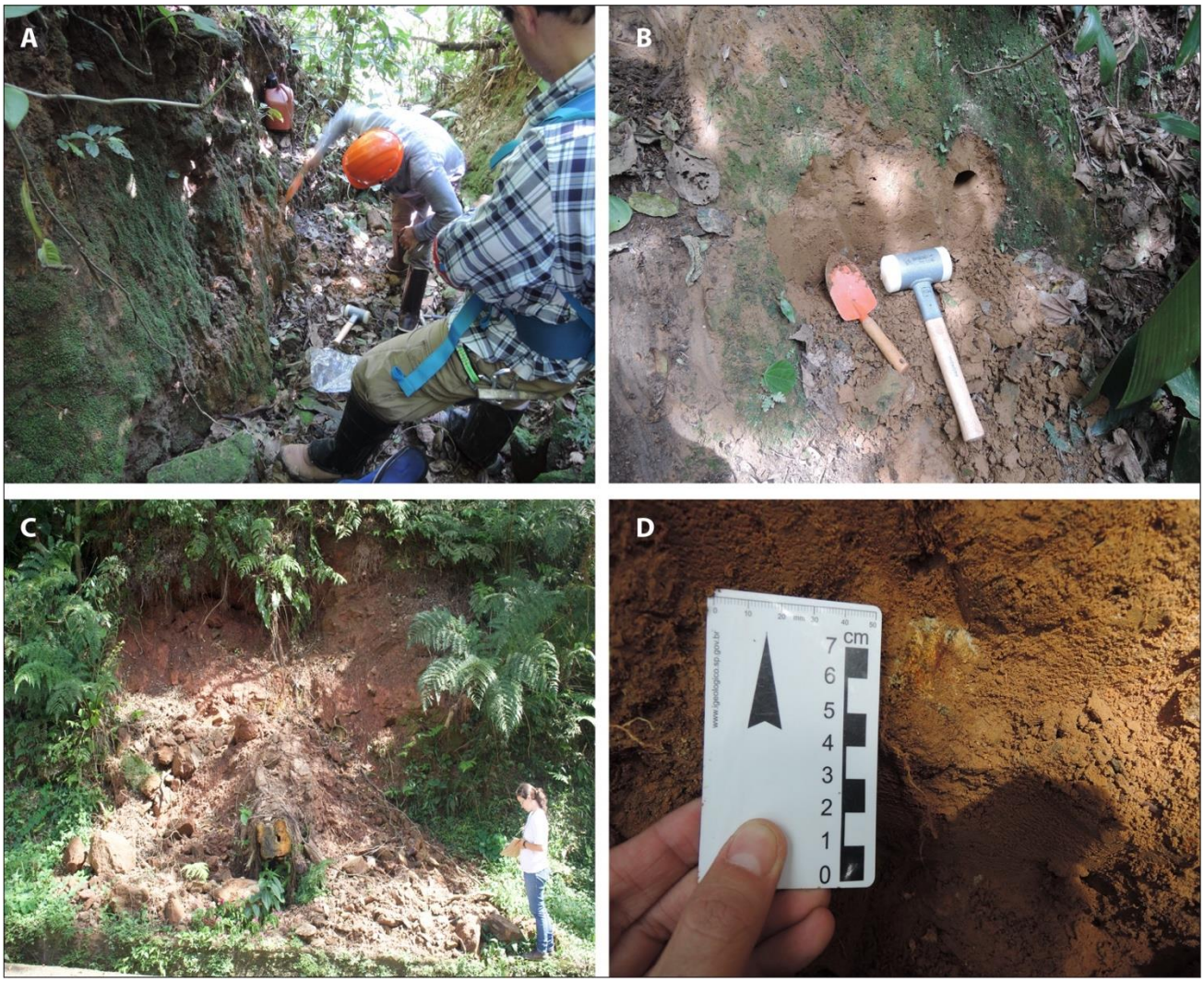

Figure 5. Soil sampling locations. A) Sampling area overview of the regolith exposure at steep slopes in the eastern portion of the Mogi watershed (UTM coordinates: X 360315 Y 7368043). B) Detail of the sampling location shown in A, a sandy-clayey soil. C) Recent shallow landslide at the hillslopes of the Rio das Pedras Catchment (Perequê watershed), comprised of gneiss boulders, woody debris and colluvium (UTM coordinates: X 352031 Y 7360097). D) Detail of the regolith above the landslide scar in C, with a sandy-clayey texture and pebble-sized blocks of weathered gneiss in the matrix.

Table 4. SHALSTAB parameters, based on Wolle and Carvalho (1989). The samples have a sandy-clayey texture and were collected at a depth of 1m (scenarios 1 and 2) and 2 m (scenario 3). UTM coordinates of the approximate sampling locations: X 351067 m E, Y 7360078 m S;and X362550 m E, Y 7368625 m S.

Parameters	Scenarios		
	1	**2**	**3**
Cohesion (Pa)	1000	3000	6000
Soil density (kN m^{-3})	17.10	15.7	14.3
Soil depth (m)	1	2	3
Internal friction angle of soil (º, degrees)	36	34	32

Table 5. SINMAP geotechnical parameters, based on soil samples from Wolle and Carvalho (1989) and rainfall data from the January 1985 event.

Parameters		Scenarios		
		1	**2**	**3**
Cohesion (dimensionless)	min	0.0406	0.992	0.1572
	max	0.0614	0.1250	0.1984
Internal friction angle of soil (º, degrees)	min	34	33	32
	max	38	37	36
Transmissivity ($m^2\ h^{-1}$)	min	0.0036	0.0036	0.0036
	max	1.0800	1.0800	1.0800
Effective rainfall ($m\ h^{-1}$)		0.0083	0.0083	0.0083
Transmissivity / effective raindfall (m)	min	0.43	0.43	0.43
	max	130.12	130.12	130.12

3.4. Performance Assessment

The Receiver Operating Characteristic (ROC) analysis is applied in model performance assessment, based on Fawcett (2006). This analysis classifies modeling results in four possible outcomes: true positive (TP), when landslide scars are observed within unstable cells; false positive (FP), when no landslide scar is observed within unstable cells; false negative (FN), when landslide scars are within stable cells; and true negative (TN), when no landslide scar is observed within stable cells (Fig. 6a).

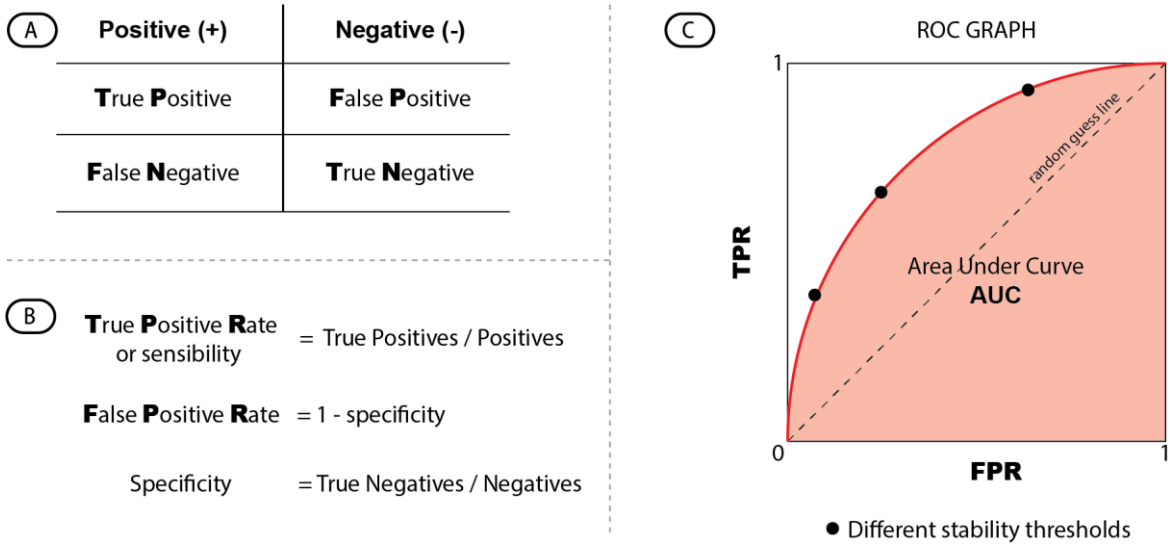

Figure 6. A) Contingency table with the four possible outcomes when assessing modeling products: true positive results (TP), false negatives (FN), false positives (FP) and true negatives (TN). B) Classifiers based on the contingency table. C) ROC analysis graph, based on the performance classifiers. Based on Fawcett (2006).

These outcomes are then used to assess modeling results, via the classifiers 'true positive rate' (TPR or sensitivity), which is the rate between TP and TP+FN, and 'false positive rate' (FPR), which is 1 minus the specificity (TN / TN+FP) (Fig. 6b). An ideal susceptibility map simultaneously maximizes the coincidence between landslides and predicted unstable areas (high TPR) and minimizes unstable areas outside known and predicted landslides (low FPR).

The TPR (y-axis) and FPR (x-axis) are then used to create the ROC graph, which depicts the trade-offs between success and error (FAWCETT, 2006). Different thresholds of stability were assumed when generating the ROC graph, in which scenarios with higher area underneath the curve (AUC) suggest more accurate performance (Fig. 6c). If a modeling scenario has classifiers beneath the random guess line, it is an indication that it performs worse than random guessing (FAWCETT, 2006).

4. Results

4.1. SHALSTAB

SHALSTAB modeling results are presented in table 6. By using the geotechnical parameters of scenario 1, 39.78% of the Perequê watershed is classified as potentially unstable (areas where $\log q/T < -2.5$), with 79.96% of the landslide scars within areas that indicate instability (Fig. 7a). At Mogi, 43.49% of the watershed is classified as potentially unstable, with 80.02% of the landslide scars in potentially unstable areas (Fig. 7a). These results indicate that when the first set of parameters is used to assess landslide susceptibility, SHALSTAB has an overall high rate of true positive results (0.8 for both watersheds) and a medium/low rate of false positive results (0.43 and 0.4 for Mogi and Perequê, respectively) (Table 7).

Using scenario 2 parameters, 36.07% of the Perequê watershed is interpreted by the model as potentially unstable, with 74.05% of the landslide scars in areas that indicate instability (Fig. 8a). 40.83% of the Mogi watershed area is interpreted as potentially unstable, with 75.85% of the landslide scars in potentially unstable areas (Fig. 8a). A high rate of true positive results (0.76 and 0.74 for Mogi and Perequê, respectively) and medium/low false positive rate (0.41 and 0.36, respectively) are observed when modelling using the geotechnical parameters of scenario 2 (Table 7), similarly to scenario 1.

When modeling using scenario 3 parameters, 16.49% of Perequê watershed is classified as potentially unstable, with 33.12% of the landslides scar in these potentially unstable areas (Fig. 9a). 21.09% of the Mogi watershed is classified as potentially unstable, with 42.24% of landslide scars in areas that indicate instability (Fig. 9a). Scenario 3 results exhibit a medium/low rate of true positive results (0.42 and 0.33 for Mogi and Perequê, respectively) and a low rate of false positive results (0.21 and 0.16, respectively) (Table 7).

Comparing the three different scenarios using the ROC analysis, scenario 1 exhibits an overall higher AUC (Fig. 10), indicating that it has a higher global accuracy (0.774 and 0.813 for Mogi and Perequê, respectively) than scenario 2 (0.757 and 0.787, respectively) and scenario 3 (0.73 and 0.77, respectively) (Table 9). This outcome suggests that scenario 1 parameters best represents slope instability at both watersheds.

4.2. SINMAP

Modeling results using SINMAP are presented in Table 8. Using scenario 1 geotechnical parameters, 42.5% of the Perequê watershed is classified as potentially unstable (SI < 1), with 75% of the landslide scars in potentially unstable areas (Fig. 7b). At Mogi, 36.20% of the watershed is classified as potentially unstable, with 71.20% of the landslide scars in areas that indicate instability (Fig. 7b). Scenario 1 exhibits a high rate of true positive results (0.71 and 0.75 for Mogi and Perequê, respectively) and a low/medium rate of false positive results (0.36 and 0.42, respectively) (Table 7).

Using scenario 2 parameters, 13.4% of the Perequê watershed is interpreted by the model as potentially unstable and 25.1% of the landslide scars are within these potentially unstable areas (Fig. 8b). 9.9% of the Mogi watershed is classified as potentially unstable, with 25.1% of the landslide scars in unstable classes. These results

indicate that scenario 2 has a low rate of true positive results (0.25 for both watersheds), as well as a low rate of false positive results (0.1 and 0.13 for Mogi and Perequê, respectively) (Table 7).

Table 6. SHALSTAB statistical summary of modeling results.

	Watershed	Scenario	Stability Classes						
			Stable	2.2	2.5 to 2.2	2.8 to 2.5	3.1 to 2.8	3.1	Chronically Unstable
Area (km²)	Mogi	1	27.01	1.58	4.19	6.35	5.84	8.55	4.49
		2	27.50	1.89	4.95	7.13	6.21	7.93	2.41
		3	36.07	3.26	6.43	6.36	3.50	2.33	0.05
	Perequê	1	12.79	2.40	2.21	2.34	1.79	2.80	4.56
		2	12.93	2.88	2.66	2.72	1.94	2.69	3.07
		3	15.70	4.80	3.63	2.51	1.11	1.02	0.12
% Area	Mogi	1	46.57	2.72	7.22	10.94	10.07	14.74	7.74
		2	47.41	3.25	8.53	12.30	10.71	13.67	4.15
		3	62.19	5.62	11.09	10.96	6.03	4.01	0.09
	Perequê	1	44.25	8.32	7.65	8.11	6.20	9.70	15.77
		2	44.75	9.98	9.21	9.41	6.73	9.32	10.61
		3	54.33	16.61	12.57	8.68	3.85	3.53	0.43
# Landslides	Mogi	1	76	32	103	149	142	234	320
		2	80	43	132	210	151	258	182
		3	191	137	282	246	106	92	2
	Perequê	1	37	21	37	35	28	53	263
		2	37	31	55	44	41	71	195
		3	52	135	130	82	31	32	12
% Landslides	Mogi	1	7.20	3.03	9.75	14.11	13.45	22.16	30.30
		2	7.58	4.07	12.50	19.89	14.30	24.43	17.23
		3	18.09	12.97	26.70	23.30	10.04	8.71	0.19
	Perequê	1	7.81	4.43	7.81	7.38	5.91	11.18	55.49
		2	7.81	6.54	11.60	9.28	8.65	14.98	41.14
		3	10.97	28.48	27.43	17.30	6.54	6.75	2.53
Density (landslides/km²)	Mogi	1	2.81	20.28	24.60	23.48	24.31	27.37	71.28
		2	2.91	22.81	26.68	29.44	24.31	32.54	75.61
		3	5.30	42.03	43.84	38.70	30.31	39.56	38.31
	Perequê	1	2.89	8.73	16.74	14.93	15.63	18.91	57.71
		2	2.86	10.75	20.66	16.18	21.08	26.36	63.59
		3	3.31	28.12	35.79	32.69	27.86	31.37	96.56

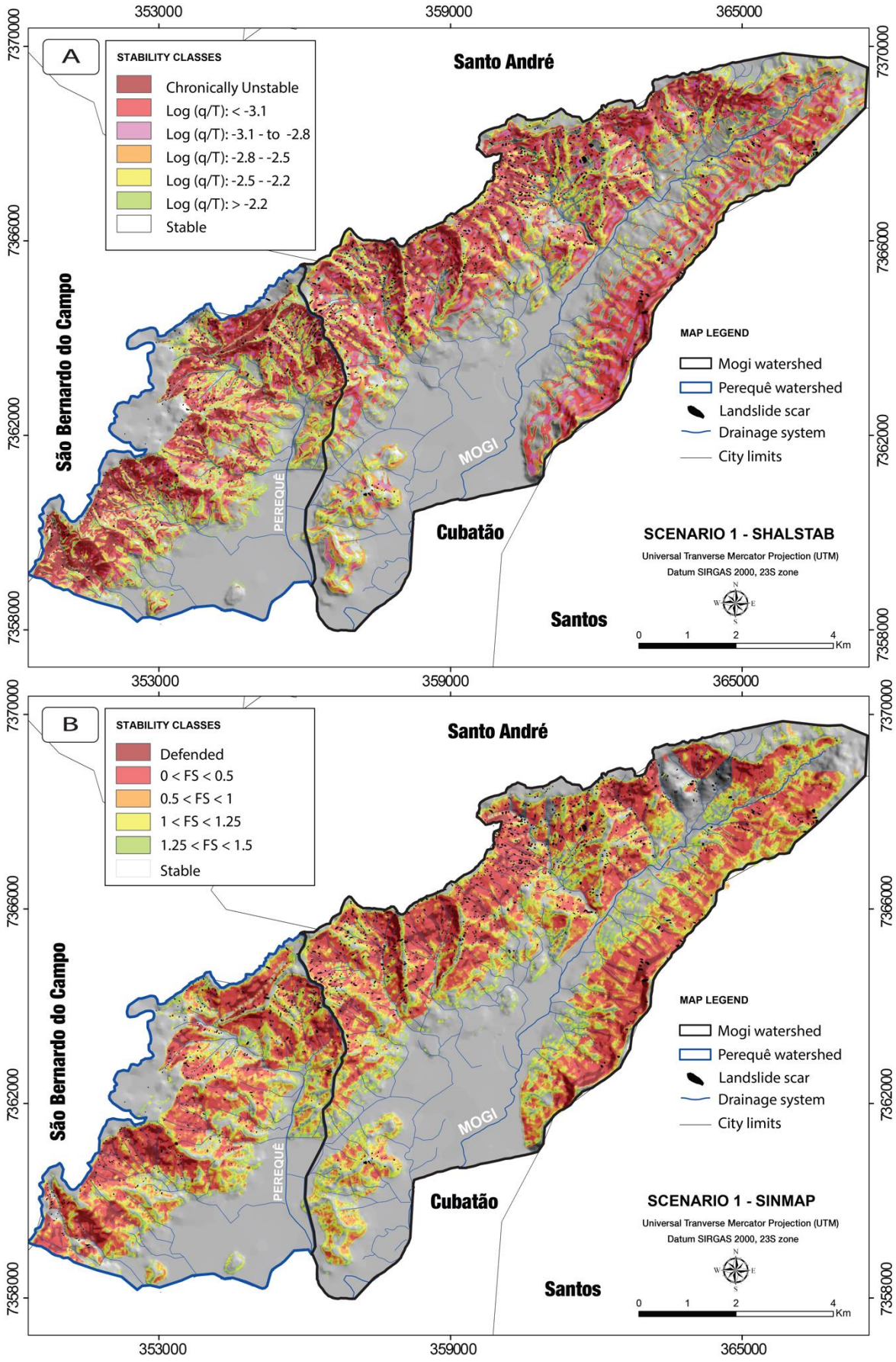

Figure 7. Stability maps using scenario 1 parameters. A) SHALSTAB. B) SINMAP.

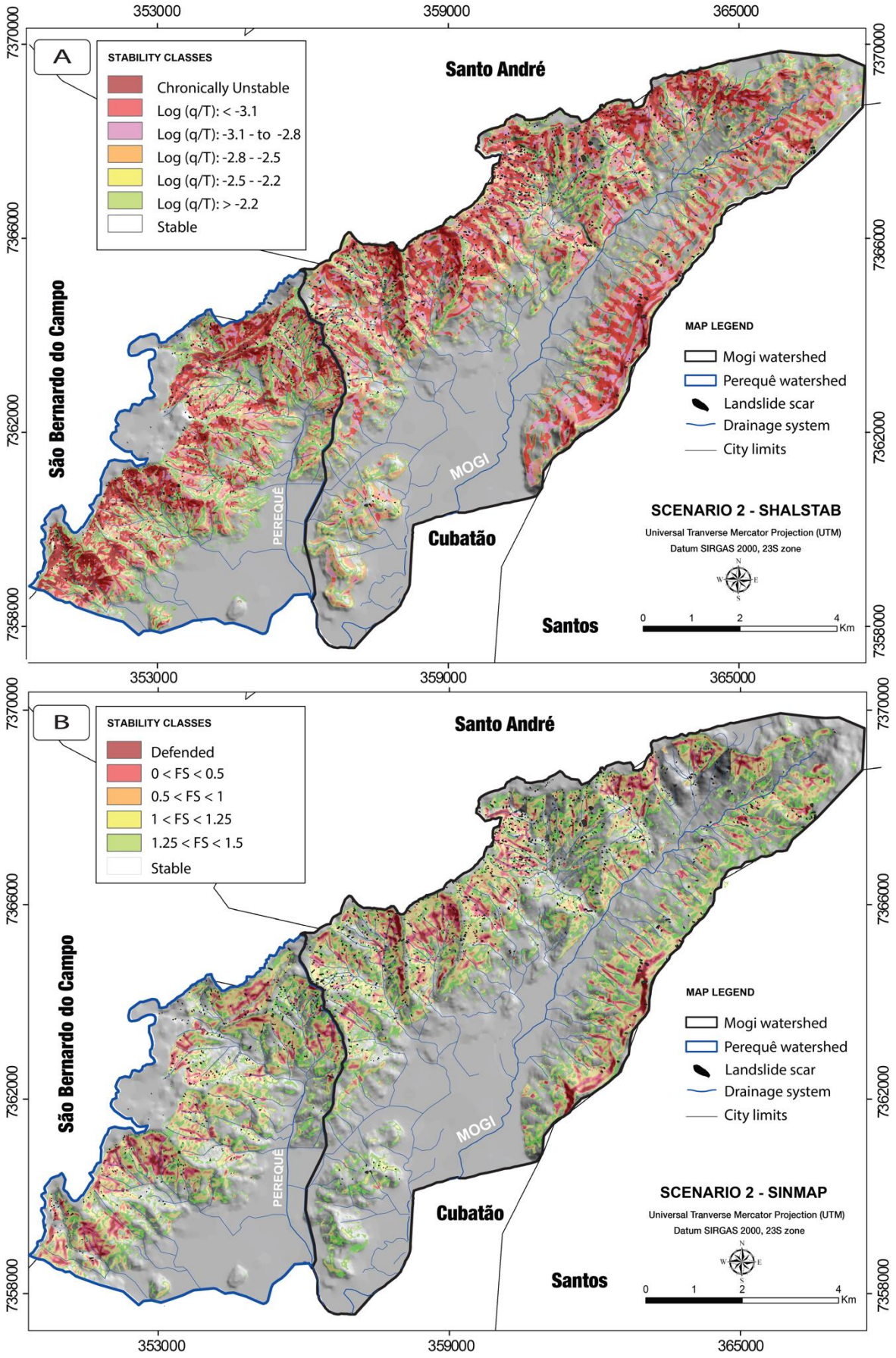

Figure 8. Stability maps using scenario 2 parameters. A) SHALSTAB. B) SINMAP.

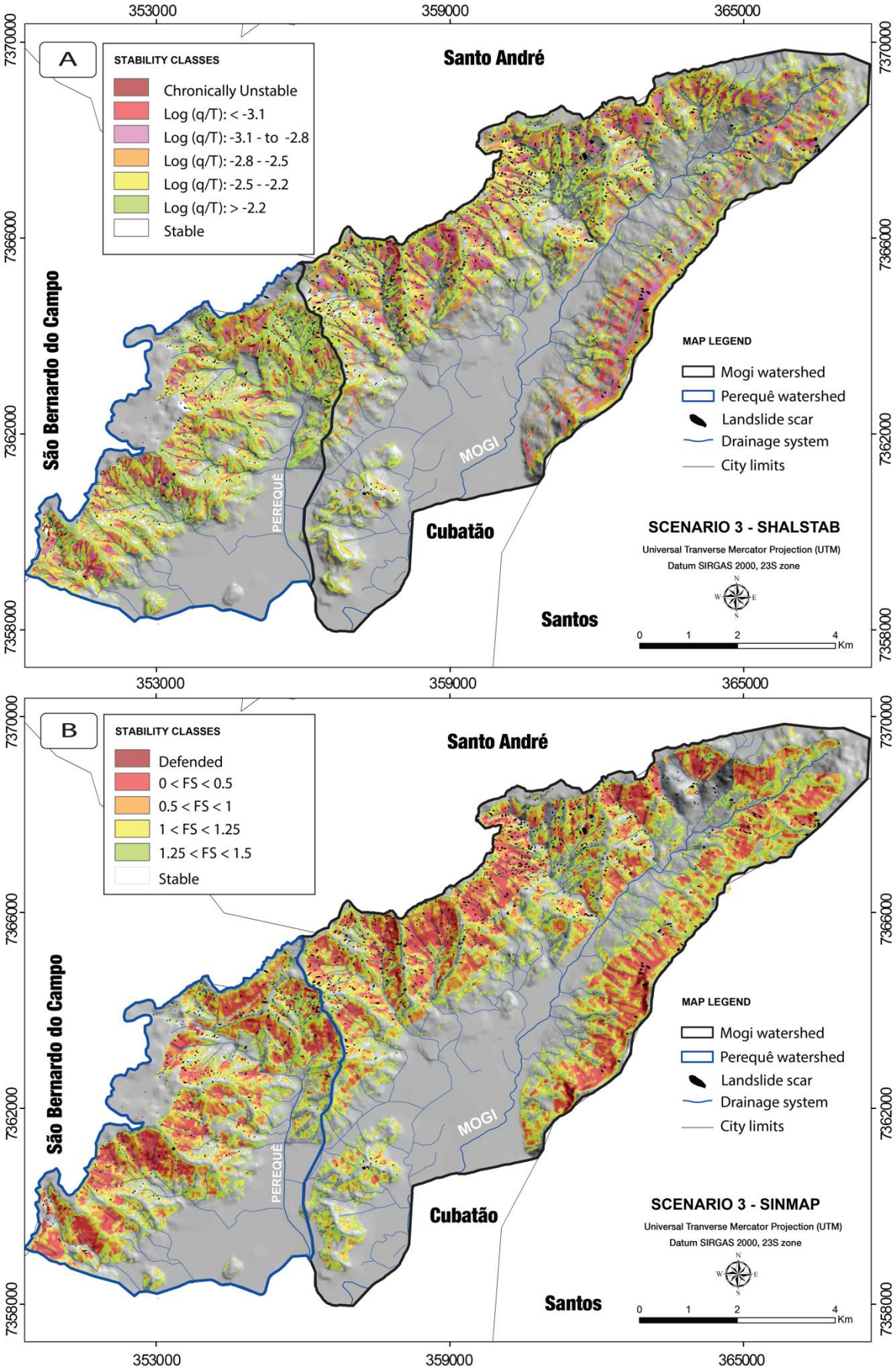

Figure 9. Stability maps using scenario 3 parameters. A) SHALSTAB. B) SINMAP.

Table 7. True Positive Rates and False Positive Rates of the three different geotechnical scenarios, according to the applied physically-based model.

Model	Scenarios	Perequê		Mogi	
		TPR	FPR	TPR	FPR
SHALSTAB	1	0.80	0.40	0.80	0.43
	2	0.74	0.36	0.76	0.41
	3	0.33	0.16	0.42	0.21
SINMAP	1	0.75	0.42	0.71	0.36
	2	0.25	0.13	0.25	0.10
	3	0.41	0.24	0.50	0.23

When applying scenario 3 parameters, 23.8% of the Perequê watershed is classified as potentially unstable, with 40.6% of the landslide scars in potentially unstable areas (Fig. 9b). 23.5% of the Mogi watershed is classified as potentially unstable, with 49.9% of the landslide scars in areas that indicate instability (Fig. 9b). Scenario 3 shows a medium rate of true positive results (0.5 and 0.4 for Mogi and Perequê, respectively) and a low rate of false positive results (0.23 and 0.24) (Table 7).

Comparing the three scenarios through the ROC analysis, scenario 1 stands out with a higher AUC than scenario 2 and 3 (Fig. 10). With scenario 1, SINMAP exhibits a higher global accuracy (0.749 and 0.725 for Mogi and Perequê, respectively), against a slightly lower performance of scenario 2 (0.747 and 0.712, respectively) and scenario 3 (0.72 and 0.7, respectively) (Table 9).

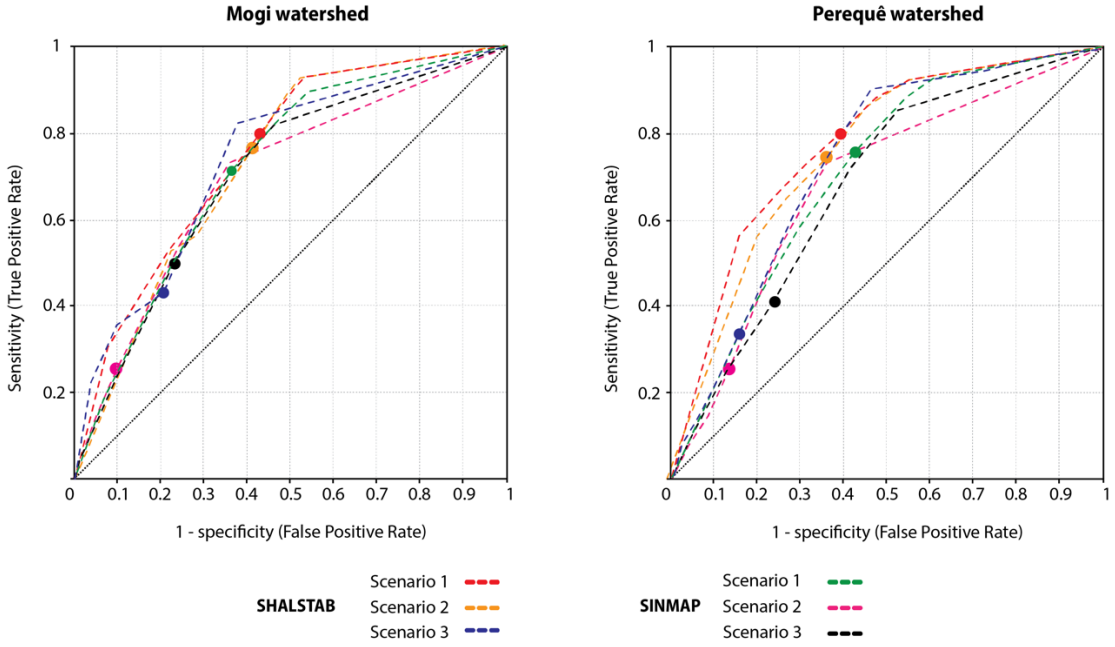

Figure 10. ROC curves for Mogi (left) and Perequê (right) watersheds. Colored dots in the curves represent the position where in SINMAP FS = 1 and in SHALSTAB log q/T = -2.5.

Table 8. Statistical summary of SINMAP modeling results.

	Watershed	Scenario	Stability Classes					
			Stable	Mod Sta	Quasi Sta	Lower	Upper	Defended
Area (km²)	Mogi	1	26.62	3.94	6.44	7.89	9.16	3.94
		2	37.06	7.02	8.18	2.67	1.45	1.62
		3	31.15	5.45	7.71	7.71	4.99	0.93
	Perequê	1	11.27	1.79	3.55	3.58	3.64	5.06
		2	18.47	3.21	3.35	1.33	1.45	1.10
		3	13.64	3.21	5.14	3.09	2.20	1.59
% Area	Mogi	1	45.90	6.80	11.10	13.60	15.80	6.80
		2	63.90	12.10	14.10	4.60	2.50	2.80
		3	53.70	9.40	13.30	13.30	8.60	1.60
	Perequê	1	39.00	6.20	12.30	12.40	12.60	17.50
		2	63.90	11.10	11.60	4.60	5.00	3.80
		3	47.20	11.10	17.80	10.70	7.60	5.50
# Landslides	Mogi	1	160	102	177	331	473	283
		2	406	308	429	157	116	110
		3	280	164	321	392	301	68
	Perequê	1	28	19	52	67	83	148
		2	106	80	111	41	30	29
		3	58	54	124	62	55	44
% Landslides	Mogi	1	10.50	6.70	11.60	21.70	31.00	18.50
		2	26.60	20.20	28.10	10.30	7.60	7.20
		3	18.03	10.70	21.00	25.70	19.70	4.50
	Perequê	1	7.05	4.79	13.10	16.88	20.91	37.28
		2	26.60	20.20	28.10	10.30	7.60	7.20
		3	14.60	13.60	31.20	15.60	13.90	11.10
Density (landslides/km²)	Mogi	1	6.01	25.86	27.49	41.96	51.62	71.75
		2	10.95	43.89	52.46	58.85	80.00	67.73
		3	8.99	30.08	41.61	50.82	60.34	73.28
	Perequê	1	2.48	10.60	14.63	18.70	22.79	29.26
		2	5.74	24.94	33.11	30.84	20.76	26.41
		3	4.25	16.83	24.10	20.05	25.04	27.68

5. Comparative analysis and discussion

SINMAP and SHALSTAB results indicate that both models have comparable degrees of success at representing landslide susceptibility at both Mogi and Perequê watersheds. SHALSTAB, however, exhibits a slightly higher global accuracy than SINMAP (Fig. 10 and Table 9), suggesting that it is more adequate for the study region.

The poorer performance of SINMAP suggests that the model fails more often than SHALSTAB in the identification of potentially unstable areas (results with an overall lower true positive rate), while maintaining similar degree of error. Using scenario 1 as an example, SHALSTAB exhibits 5% more true positive results, with a 2% lower false positive rate compared to SINMAP at the Perequê watershed. At Mogi, while true positive results using SHALSTAB is 10% higher, the model also has a 7% higher false positives rate, resulting in a more similar performance with SINMAP (Table 9). SHALSTAB, nonetheless, exhibits a higher global accuracy for both watersheds in all geotechnical scenarios.

Table 9: Global accuracy of each scenario and model, represented by the area under the curve (AUC) of the ROC curve. The higher the AUC, the better the performance.

Area under the curve (AUC)						
Model	**Mogi**			**Perequê**		
	Sce 1	**Sce 2**	**Sce 3**	**Sce 1**	**Sce 2**	**Sce 3**
SHALSTAB	0.774	0.757	0.729	0.813	0.787	0.767
SINMAP	0.749	0.747	0.715	0.725	0.712	0.701

Soil cohesion and thickness are the main differences between the different scenarios and, while the disparity in global accuracy between them is not substantial, the results of scenario 3 (and 2 in SINMAP) are much more conservative than scenario 1. We can observe that scenario 3 considerably underestimates potentially unstable areas in both watersheds. In total, 0.1% of Mogi and 0.43% of Perequê watershed is classified as 'Chronically unstable' in scenario 3 using SHALSTAB, with only 2 and 12 landslide scars in this class, respectively. In SINAMP, only 1.6% of the Perequê watershed is in the 'Defended' class (SINMAP), with 44 landslide scars. While scenario 2 did not provide underestimated results using SHALSTAB, in SINMAP only 2.8% of the Mogi watershed is classified as 'Defended', encompassing 110 landslide scars.

'Chronically unstable' and 'Defended' areas are associated to regions of bedrock outcrops (Fig. 11a) and/or areas that are unstable even without precipitation or run-off, such as those with steep slopes (>40º) and thin soil cover (0 – 1 m depth) (MONTGOMERY; DIETRICH, 1994; DIETRICH *et al*., 2001; MICHEL *et al*., 2015). During our field campaigns, period without recent records of heavy rainfall events, more than 10 landslides scars were observed in steep areas (e.g., Fig. 5 c and 11b) that would fall under the most extreme classes of the models. When the dimension of the 1985 landslide event is considered, it is even more evident how the lowest stability class should account for more of the study area and encompass more landslide scars than it does when scenario 2 and, especially, 3 are employed.

The more conservative performance of both scenarios 3 and 2 highlights how the input parameters impact on the susceptibility scenarios given by the models. The use of geotechnical parameters in which the average depth of the slope failure is > 2 m and cohesion values are higher results in a larger percentage of the study region being classified as stable, which may not be representative of the real conditions of the hillslopes. Therefore, a > 2 m depth for the failure surface of shallow landslides is likely overestimated, as well as high cohesion values (> 3000 Pa) for regolith derived from gneiss and granitoid rocks.

Although tropical soil is heterogeneous and anisotropic by nature, representing a challenge to consider and characterize during modeling (CAMPOS *et al*., 1992; BRUGGER *et al*., 1997; GERSCOVITCH *et al*., 2006), our results indicate that the soil of the hillslopes of Mogi and Perequê exhibits a general trend of low cohesion (sandy soils) and a shallow failure depth (ca. 1m). This trend can be observed when using both models, in which the scenarios with progressive lower values of cohesion, higher values of internal friction angle and shallower depths of rupture show superior performances. A single set of parameters for a broad region, however, can potentially generalize the geotechnical behavior of a region, representing a drawback for detailed studies. Nonetheless, as often regional scale studies demand fewer financial investments, the definition of a general geotechnical behavior for an area is useful as a starting point for hazard assessments and the application of other physically-based models.

One great challenge when working at Serra do Mar, especially in a broader scale, is the challenges associated to systematic sampling and fieldwork logistics. Especially for Mogi watershed, the steep slopes, dense forest and not very clear trails difficult the access, often posing danger. Despite the challenges, fieldwork is extremely important to analyze and confirm the geomorphological and geotechnical characteristics of the study region. Fieldwork can also support the compartmentalization of a region according to geology and landform characteristic, which, combined with systematic sampling, should improve the representativeness of modeling results and is recommended for future studies in the region. Such systematic sampling and fieldwork analysis is simpler and safer to achieve in smaller and less remote areas, such as the sub-catchments of the Perequê watershed.

Comparative studies between different techniques, albeit with similar core parameters, highlight how site-specific the application of physically-based models are and how the best-fit model for a region depends largely on the available data, both related to soil and topography. Comparative analyses are, therefore, fundamental in ensuring the reliability of slope stability representation in a region, supporting urban-planning studies, as well as risk and hazard assessments.

Similar comparative studies have been made worldwide and the results greatly vary according to region and scale. The literature generally suggests SHALSTAB as the most recommended for smaller and fine detail studies, while SINMAP the most suited for regional scale ones (areas over 20 km^2). Such conclusions can be observed in the studies of Meisina and Scarabelli (2007), Andriola *et al*. (2009), Pradhan and Kim (2014), which have also compared both models. More recently, Michel *et al*. (2014) and Cabral and Reis (2020) have also concluded that SHALSTAB is the best-fit for small catchments at different areas of the Serra do Mar mountain range.

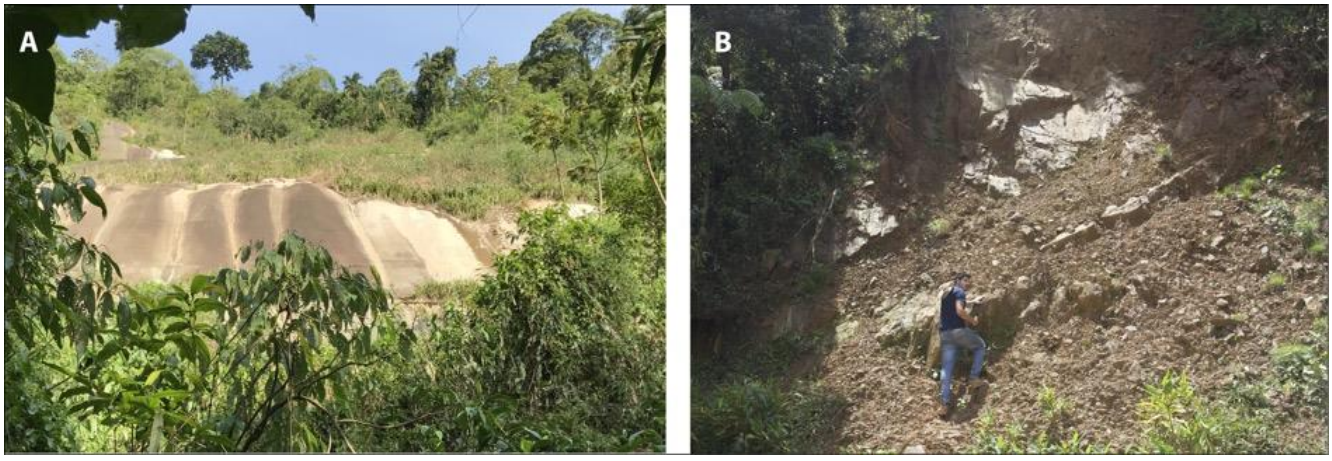

Figure 11. A) Bedrock exposed area (UTM Coordinates: 362258 m E; 7364004 m N). B) Shallow landslide scar in steep slope (>40º). Soil depth in steeper slopes ranges from 0 to 1 m (UTM Coordinates: 352780 m E; 7360811 m N).

While SHALSTAB requires high-resolution topographic data (DIETRICH *et al*., 2001), SINMAP can potentially be useful in areas where data resolution is not very refined (e.g., > 10 m resolution DEM) (LOPES *et al*., 2007). Sizioli *et al*. (2013) compared four different stability models in alpine catchments in Italy, with a coarser DEM (10m) and concluded that SINMAP performed better than SHALSTAB, even in relatively smaller watersheds (10 to 15 km²). Furthermore, Cardozo *et al.* (2018) and Affandani and Kusratmoko (2019) also found that SINMAP is adequate when applied in smaller watersheds (> 5 km²), although in these last two studies a comparative analysis with SHALSTAB was not performed.

Due to the probabilistic nature, which admits uncertainty over the input parameters, SINMAP can be advantageous for large areas (LOPES *et al*., 2007; THIEBES *et al*., 2016), as it is also suggested by the relative better performance of SINMAP at the larger Mogi watershed than at Perequê. The overall results of our study, however, show a superior performance of SHALSTAB when applied at the region of Cubatão in the Serra do Mar mountain range.

6. Conclusion

This study compared the performance of the physically-based models SHALSTAB and SINMAP in the landslide susceptibility assessment of the watersheds Mogi and Perequê, located at the Serra do Mar Mountain Range. The 1985 landslide event was chosen to calibrate model performance, due to its wide spatial distribution across both watersheds and due to the availability of high-quality data. The comparative performance analysis was made through the Receiver Operating Characteristics (ROC) analysis, a simple and effective way to assess modeling results via the relationship between success (true positive) and error (false positive) of the results.

SHALSTAB emerges as the model that best represents landslide susceptibility at both watersheds, due to its higher concentration of landslide scars in unstable areas (true positive results) and higher global accuracy (the rate between true positive and false positive results). Even though SINMAP had similar degree of success as SHALSTAB, it was slightly less accurate and it failed more often to identify unstable areas in the landform.

Three different geotechnical scenarios were considered during modeling, the first one (1) with lowest values of colluvial samples and the second (2) with average values and third (3) with the highest values. Scenario 1 results were more similar to the landslide event of 1985, showing higher true positive results and accuracy. Scenario 3 was more conservative, often failing to identify potentially unstable areas, which is not ideal for susceptibility studies. Scenario 2 performed similarly to scenario 1, which suggest that the landslides at the study region have a failure depth of up to 2 m and occur in sandy regolith (with low cohesion values and higher internal friction angle).

Future comparative studies of physically-based models are recommended to be applied in smaller areas, where a more detailed geological mapping is possible and a higher sampling density is easier to achieve - especially at Serra do Mar where access is challenging. Nonetheless, comparative performance studies in regional scales are extremely important in hazard assessment and urban planning studies in mountain regions, providing an outlook in how to proceed in more detailed assessments.

Contribuições dos Autores: Concepção - V.C. Cabral, F.A.G.V Reis, C.M. Mendoza; Metodologia – V.C. Cabral, C.M Mendoza, A. Oliveira; Preparação de dados e resultados: V.C. Cabral; Discussão: V.C. Cabral, F.A.G.V Reis, C.M. Mendoza, A. Oliveira. Todos os autores leram e concordaram com a versão publicada do manuscrito.

Financiamento: Esta pesquisa foi financiada em parte pelo Conselho Nacional de Desenvolvimento Científico e Tecnológico – CNPq, pela concessão de bolsa de mestrado ao primeiro autor.

Agradecimentos: Os autores agradecem ao Dr. Fernando Mazo D'Affonseca pelas sugestões durante o desenvolvimento desta pesquisa, assim como aos dois revisores anônimos, que contribuíram com a melhora da clareza do manuscrito.

Conflito de Interesse: Os autores declaram não haver conflito de interesse.

Referências

1. AFFANDANI, A.Y.; KUSRATMOKO, E. Landslide susceptibility mapping using SINMAP method in a small hilly area: case study in Cibanteng Village, West Java. **IOP Conference Series: Earth Environmental Sciences**, v. 311:012027, 2019. Doi: 10.1088/1755-1315/311/1/012027
2. AHERN, M.; KOVATS, R.S.; WILKINSON, P.; FEW, R.; MATTHIES, F. Global health impacts of floods: Epidemiologic evidence. **Epidemiologic Reviews**, v. 27, p. 36–46, 2005. Doi: 10.1093/epirev/mxi004
3. ALEOTTI P.; CHOWDHURY, R. Landslide hazard assessment: summary review and new perspectives. **Bulletin of Engineering Geology and Environment**, v. 58, p. 21–44, 2019. Doi: 10.1007/s100640050066
4. ALVIOLI, M.; BAUM, R. Parallelization of the TRIGRS model for rainfall-induced landslides using the message-passing interface. **Environmental Modelling & Software**, v. 81, p. 122-135, 2016. Doi: 10.1016/j.envsoft.2016.04.002
5. ANDRIOLA, P.; CHIRICO, G.B.; DE FALCO, M.; CRESCENZO, G.; SANTO, A. A comparison between physically based models and a semiquantitative methodology for assessing susceptibility to flowslides triggering in pyroclastic deposits of Southern Italy. **Geografia Fisica e Dinamica Quaternaria**, v. 32, p. 213-26, 2009.
6. AVILA, F. F.; ALVALA, R. C. S.; MENDES, R. M.; AMORE, D. The influence of land use/land cover variability and rainfall intensity in triggering landslides: a back-analysis study via physically based models. **Natural Hazards**, v. 104, p. 1, 2020. Doi: 10.1007/s11069-020-04324-x
7. BAUM, R.L.; SAVAGE, W.Z.; GODT, J.W. TRIGRS- a Fortran Program for Transient Rainfall Infiltration and Grid-based Regional Slope-stability Analysis. **Open-File Report**, p. 35, 2002.
8. BEL, C.; LIÉBAULT, F.; NAVRATIL, O.; ECKERT, N.; BELLOT, H.; FONTAINE, F.; LAIGLE, D. Rainfall control of debris-flow triggering in the Réal Torrent, Southern French Alps. **Geomorphology**, v. 291, p. 17-32, 2016. Doi: 10.1016/j.geomorph.2016.04.004
9. BEVEN, K.J.; KIRKBY, M.J. A Physically based variable contributing area model of basin hydrology. **Hydrological Sciences Bulletin,** v. 24, p. 43-69, 1979. Doi: 10.1080/02626667909491834
10. BRUGGER, P.J.; EHRLICH, M.; LACERDA, W.A. Movements, piezometric level and rainfall at two natural slopes. In: Conferência Brasileira Sobre Estabilidade De Encostas, 2, 1997, Rio de Janeiro. **Anais...**. Rio de Janeiro. 1997. p.13-20.
11. CABRAL, V.; REIS, F.; VELOSO, V.; CORREA, C.; MENDOZA, C.; ALMEIDA, N.; GIORDANO, L. Assessment of the influence of rainfall and landform on landslide initiation using physiographic compartmentalization. **Anuário do Instituto de Geociências**, v. 42, n. 2, p. 432- 455, 2019. Doi: 10.11137/2019_2_407_420
12. CABRAL, V.C.; REIS, F.A.G.V. Assessment of Shallow Landslides Susceptibility Using SHALSTAB and SINMAP at Serra Do Mar, Brazil. In: GUZZETTI, F.; MIHALIĆ ARBANAS, S.; REICHENBACH, P.; SASSA, K.; BOBROWSKY, P.T.; TAKARA K. (eds) **Understanding and Reducing Landslide Disaster Risk**. World Landslide Forum, 2020, ICL Contribution to Landslide Disaster Risk Reduction. Springer, Cham. Doi: 10.1007/978-3-030-60227-7_28
13. CAMPOS, T.M.P.; VARGAS JR, E.A.; EISENSTEIN, Z. Considerações sobre o processo de instabilização de encostas em solos não-saturados no Rio de Janeiro. In: Conferência Brasileira Sobre Estabilidade De Encostas, 1, 1992, Rio de Janeiro. **Anais....** Rio de Janeiro. 1992. p. 741-755.
14. CAPPARELLI, G.; VERSACE, P. FLaIR and SUSHI: two mathematical models for early warning of landslides induced by rainfall. **Landslides**, v. 8, p. 67–79, 2011. Doi: 10.1007/s10346-010-0228-6
15. CARDOZO, C.P.; LOPES, E.S.S.; MONTEIRO, A.M.V. Calibration of physically based slope-stability models: a case study in Nova Friburgo (Rio de janeiro, Brazil). **Geociências**, v. 38, n. 2, p. 535-548, 2019.
16. CLAESSENS, L.; HEUVELINK, G.B.M.; SCHOORL, J.M.; VELDKAMP, A. DEM resolution effects on shallow landslide hazard and soil redistribution modeling. **Earth Surface Processes and Landforms**, v. 30, n. 4, p. 461-477, 2005. Doi: 10.1002/esp.1155
17. CROSTA, G. Introduction to the special issue on rainfall-triggered landslides and debris flows. **Engineering Geology**, v. 73, n. 3-4, p. 191-192, 2004. Doi: 10.1016/j.enggeo.2004.01.004
18. CRUDEN, D.M. A simple definition of a landslide. **Bulletin of the International Association of Engineering Geology**, v. 43, n. 1, p. 27–29, 1991. Doi: 10.1007/BF02590167

19. DIETRICH, W. E.; ASUA, R.R.; TRSO, M. **A validation study of the shallow slope stability model, SHALSTAB, in forested lands of Northern California**. Department of Geology and Geophysics University of California, Berkeley, 1998.
20. DIETRICH, W.E.; BELLUGI, D.; ASUA, R. Validation of the shallow landslide model, SHALSTAB, for forest management**.** In: WIGMOSTA, M.S.; BURGES, S.J. (Eds.) **Land use and watersheds: human influence on hydrology and geomorphology in urban and forest areas.** AGU, Washington DC, 2001, v. 2, p. 195–227.
21. DOURADO, F.; ROIG, H. Mapas de susceptibilidade a escorregamentos rasos, usando os modelos SHALSTAB e SINMAP, da Bacia do Rio Pequequer – Teresópolis – RJ. **Cadernos de Estudos Geoambientais – CADEGEO**, v. 4, n. 1, p. 56-66, 2013.
22. FAWCETT, T. An introduction to ROC analysis. **Pattern Recognition Letters**, v. 27, n. 8, p. 861–874, 2016. Doi: 10.1016/j.patrec.2005.10.010
23. FERNANDES, N.F.; GUIMARÃES, R.F.; GOMES, R.A.T.; VIEIRA, B.C.; MONTGOMERY, D.R.; GREENBERG, H. Geomorphological conditions of landslides: evaluation of methodologies and application of predictive model of susceptible areas. **Revista Brasileira de Geomorfologia**, v. 2, n. 1, p. 51–71, 2001.
24. GERSCOVICH, D.M.S.; CAMPOS, T.P.P.; VARGAS JR, E.A. On the evaluation of unsaturated flow in a residual soil slope in Rio de Janeiro, Brazil. **Engineering Geology**, v. 88, p. 23 – 40, 2006. Doi: 10.1016/j.enggeo.2006.07.008
25. GIANNECCHINI, R.; GALANTI, Y.; AVANZI, G.D.; BARSANTI, M. Probabilistic rainfall thresholds for triggering debris flows in a human-modified landscape. **Geomorphology**, v. 257, p. 94- 107, 2016. Doi: 10.1016/j.geomorph.2015.12.012
26. GODT, J.; BAUM, R.; SAVAGE, W.; SALCIARINI, D.; SCHULZ, W.; HARP, E. Transient deterministic shallow landslide modeling: Requirements for susceptibility and hazard assessments in a GIS framework. **Engineering Geology**, v. 102, n. 3–4, p. 214–226, 2008. Doi: 10.1016/j.enggeo.2008.03.019
27. GOETZ, J.; GUTHRIE, R.; BRENNING, A. Integrating physical and empirical landslide susceptibility models using generalized additive models. **Geomorphology**, v. 129, n. 3-4, p. 376-386, 2011. Doi: 10.1016/j.geomorph.2011.03.001
28. GOMES, R.A.T. **Modelagem de previsão de movimentos de massa a partir da combinação de modelos de escorregamentos e corridas de massa**. Tese (Doutorado em Geografia) Universidade Federal do Rio de Janeiro, Rio de Janeiro. 2006. 180 p.
29. GRAMANI, M.F. **Caracterização geológica-geotécnica das corridas de detritos ("Debris Flows") no Brasil e comparação com alguns casos internacionais**. Dissertação (Mestrado em Engenharia), Universidade de São Paulo, São Paulo. 2001. 372 p.
30. GUIDICINI, G.; LWASA, O.Y. Tentative correlation between rainfall and landslides in a humid tropical environment. **Bulletin of the International Association of Engineering Geology**, v. 16, p. 13-20, 1977. Doi: 10.1007/BF02591434
31. GUIDICINI, G.; NIEBLE, C.M. **Estabilidade de Taludes Naturais e de Escavação**. São Paulo: Editora da USP, 1984. 216 p.
32. GUIMARÃES, R.F.; MONTGOMERY, D.R.; GREENBERG, H.M.; FERNANDES, N.F.; GOMES, R.A.T.; CARVALHO JR, O.A.P. Parameterization of soil properties for a model of topographic controls on shallow landsliding: application to Rio de Janeiro. **Engineering Geology**, v. 69, p. 99-108, 2003. Doi: 10.1016/S0013-7952(02)00263-6
33. GUIMARÃES, R.F.; GOMES, R.A.T.; CARVALHO JÚNIOR, O.A.; MARTINS, E.S.; FERNANDES, N.F. Análise temporal das áreas suscetíveis a escorregamentos rasos no Parque Nacional da Serra dos Órgãos (RJ) a partir de dados pluviométricos. **Revista Brasileira de Geociências**, v. 39, p. 192–200, 2009. Doi: 10.25249/0375-7536.2009391190198
34. GUZZETI, F.; CARRARA, A.; CARDINALI, M.; REICHENBACH, P. Landslides hazard evaluation: a review of current techniques and their application in a multi-scale study, Central Italy. **Geomorphology**, v. 31, p. 181-216, 1999. Doi: 10.1016/S0169-555X(99)00078-1
35. HALLEGATTE, S.; GREEN, C.; NICHOLLS, R.J.; CORFEE-MORLOT, J. Future flood losses in major coastal cities. **Nature Climate Change**, v. 3, p. 802–806, 2013. Doi: 10.1038/nclimate1979
36. HASUI, Y. Sistema Orogênico Mantiqueira. In: **Geologia do Brasil**. São Paulo: Beca-BALL Ltda., 2012. 900 p.
37. IPT (1986) **Programa Serra do Mar – levantamentos básicos nas folhas de Santos e Riacho Grande, Estado de São Paulo**. Publicação IPT nº 23.394(2), 120p.
38. KANJI, M.A.; CRUZ, P.T.; MASSAD, F. Debris flow affecting the Cubatão oil refinery, Brazil. **Landslides**, v. 5, n. 1, p. 71-82, 2007. Doi: 10.1007/s10346-007-0110-3
39. KEEFER, D.K.; LARSEN, M.C. GEOLOGY: Assessing Landslide Hazards. **Science**, v. 316, n. 5828, p. 1136-1138, 2007. Doi: 10.1126/science.1143308
40. KNAPP, A.K.; BEIER, C.; DAVID, D. et al. Consequences of More Extreme Precipitation Regimes for Terrestrial Ecosystems. **BioScience**, v. 58, n. 9, p. 811-821, 2008. Doi: 10.1641/B580908
41. KOBIYAMA, M.; MICHEL, G.; ENGSTER, E.; PAIXÃO, M. Historical analyses of debris flow disaster occurrences and of their scientific investigation in Brazil. **Labor e Engenho**, v. 9, n. 4, p.76, 2015. Doi: 10.20396/lobore.v9i4.8639477

42. KONIG, T.; KUX, HERMANN J. H.; MENDES, R. M. Shalstab mathematical model and WorldView-2 satellite images to identification of landslide-susceptible areas. **Natural Hazards**, v. 98, p. 1-23, 2019. Doi: 10.1007/s11069-019-03691-4
43. LISTO, F.L.R. **Propriedades geotécnicas dos solos e modelagem matemática de previsão a escorregamentos transnacionais rasos**. Tese (Doutorado em Geografia), Universidade de São Paulo, São Paulo, 2015. 167 p.
44. LIU, C.; HU, M.; LU, P.; LI, W.; SCAIONI, M.; WU, H.; YE, B. Assessment of regional shallow landslide stability based on airborne laser scanning data in the Yingxiu area of Sichuan Province (China). **European Journal of Remote Sensing**, v. 49, n. 1, p. 835-860, 2016. Doi: 10.5721/EuJRS20164944
45. LIU, C.N.; WU, C.C. Integrating GIS and stress transfer mechanism in mapping rainfall-triggered landslide susceptibility. **Engineering Geology**, v. 101, n. 1–2, p. 60–74, 2008. Doi: 10.1016/j.enggeo.2008.04.003
46. LOPES, E.S.S.; RIEDEL, P.S.; BENTS, C.M.; FERREIRA, M.V.; NALETO, J.L.C. Inventário de escorregamentos naturais em banco de dados geográfico – análise dos fatores condicionantes na região da Serra de Cubatão – SP. In: XIII Simpósio Brasileiro de Sensoriamento Remoto, 13., 2007, Florianópolis. **Anais…** São José dos Campos: INPE, 2007. p. 2785-2796.
47. MASSAD, F.; CRUZ, P.T.; KANJI, M.A. Comparison between estimated and mensured debris flow discharges and volume of sediments. In: II Conferência Brasileira sobre Estabilidade de Encostas/2nd Pan- American Symposium on Landslides. **Anais...** Rio de Janeiro, 1997, p. 213–222
48. MASSAD, F.; CRUZ, P.T.; KANJI, M.A.E.; ARAUJO FILHO, H.A. **Characteristics and volume of sediment transported in debris flows in Serra do Mar, Cubatão, Brasil**. In: International workshop on debris flow disaster of December. Venezuela, Caracas, 2000.
49. MEISINA, C.; SCARABELLI, S. A comparative analysis of terrain stability models for predicting shallow landslides in colluvial soils. **Geomorphology**, v. 87, p. 207–223, 2007. Doi: 10.1016/j.geomorph.2006.03.039
50. MICHEL, G.; KOBIYAMA, M.; GOERL, R.F. Comparative analysis of SHALSTAB and SINMAP for landslide susceptibility mapping in the Cunha River basin, southern Brazil. **Journal of Soils and Sediments**, v. 14, n. 7, p. 1266–1277, 2014. Doi: 10.1007/s11368-014-0886-4
51. MICHEL, G.; GOERL, R.; KOBIYAMA, M. Critical rainfall to trigger landslides in Cunha River basin, southern Brazil. **Natural Hazards**, v. 75, n. 3, p. 2369-2384, 2015. Doi: 10.1007/s11069-014-1435-6
52. MOINE, M.; PUISSANT, A.; MALET, J.P. Detection of landslides from aerial and satellite images with a semi-automatic method. Application to the Barcelonnette basin (Alpes-de-Hautes- Provence, France). In: Landslide Processes Conference - From Geomorphologic Mapping to Dynamic Modeling: A Tribute to Dr. Theo Van Asch, 2009, France. **Anais…** Strasbourg, France, 2009. p. 63-68.
53. MONTGOMERY, D.; DIETRICH, W. A physically based model for the topographic control on shallow landsliding. **Water Resources Research**, v. 30, n.4, p. 1153-1171, 1994. Doi: 10.1029/93WR02979
54. MORRISSEY, M.M.; WIECZOREK, G.F.; MORGAN, B.A. **A comparative analysis of hazard models for predicting debris flows in Madison Country, Virginia**. Relatório Técnico nº 01-0067, U.S. Geological Survey, 2001, 28 p.
55. NERY, T.D.; VIEIRA, B.C. Susceptibility to shallow landslides in a drainage basin in the Serra do Mar, São Paulo, Brazil, predicted using the SINMAP mathematical model. **Bulletin of Engineering Geology and Environment**, v. 74, n. 2, p. 369-378, 2014. Doi: 10.1007/s10064-014-0622-8
56. NIKOLOPOULOS, E.I.; BORGA, M.; CREUTIN, J.D.; MARRA, F. Estimation of debris flow triggering rainfall: Influence of rain gauge density and interpolation methods. **Geomorphology**, v. 243, p. 40–50, 2015. Doi: 10.1016/j.geomorph.2015.04.028
57. PACK, R.T.; TARBOTON, D.G.; GOODWIN, C.N. The SINMAP approach to terrain stability mapping. In: Congress of The International Association of Engineering Geology, 8, 1998, Vancouver. **Anais…** British Columbia, Canada, 1998. 25p.
58. PETLEY, D. Global patterns of loss of life from landslides. **Geology**, v. 40, n. 10, p. 927-930, 2012. Doi: 10.1130/G33217.1
59. PRADHAN, A.M.S.; KIM, Y. Relative effect method of landslide susceptibility zonation in weathered granite soil: a case study in Deokjeok-ri Creek, South Korea. **Natural Hazards**, v. 72, n. 2, p. 1189-1217, 2014. Doi: 10.1007/s11069-014-1065-z
60. PRIETO, C. C.; MENDES, R. M.; SIMOES, S. J. C.; NOBRE, C. A. Comparação entre a aplicação do modelo Shalstab com mapas de suscetibilidade e risco de deslizamentos na bacia do córrego Piracuama em Campos do Jordão - SP. **Revista Brasileira de Cartografia**, v. 69, p. 71-87, 2017.
61. RAFAELLI, S.G.; MONTGOMERY, D.R.; GREENBERG, H.R. A comparison of thematic mapping of erosional intensity to GIs-driven process models in an Andean drainage basin. **Hydrological Processes**, v. 244, p. 33-42, 2001. Doi: 10.1016/S0022-1694(00)00419-4

62. REGINATTO, G.M.P. **Caracterização de movimentos de massa na bacia hidrográfica do Rio Cunha, Rio dos Cedros-SC, com ênfase em escorregamentos translacionais**. Dissertação (Mestrado em Engenharia), Universidade Federal de Santa Catarina, 2013. 200 p.
63. ROSOLEM, G.P.N.; ROSENFELDT, Y.A.Z.; LOCH, C.; HIGASHI, R.A.R. The influence of cartographic's Products Quality on Analysis of Translational Landslides through SHALSTAB Model Application. **Revista Brasileira de Cartografia**, v. 69, n. 1, p. 43-60, 2017. Doi: 10.21094/rg.2017.015
64. SBROGLIA, R.M.; REGINATTO, G.M.P; HIGASHI, R.A.R.; GUIMARÃES, R.F. Mapping susceptible landslide areas using geotechnical homogeneous zones with different DEM resolutions in Ribeirão Baú basin, Ilhota/SC/Brazil. **Landslides**, v. 15, n. 10, p. 2093-2106, 2018. Doi: 10.1007/s10346-018-1052-7
65. SCHUSTER, R.L. Socioeconomic significance of landslides. In: TURNER, A.K.; SCHUSTER, R.L. (Eds.) **Landslides: Investigation and Mitigation**. National Academy Press, Washington D.C.: 1996, p. 12–35.
66. SEEFELDER, C. L. N. **Estudo da influência dos parâmetros hidrogeológicos na análise de susceptibilidade à escorregamentos rasos por meio de modelo de estabilidade de encostas**. Tese de Doutorado em Tecnologia Ambiental e Recursos Hídricos, Departamento de Engenharia Civil e Ambiental, Universidade de Brasília, Brasília, DF, 2017, 212p.
67. SESTINI, M.F. **Variáveis Geomorfológicas no Estudo de Deslizamentos em Caraguatatuba-SP utilizando imagens TM-LANDSAT e SIG**. Dissertação (Mestrado em Sensoriamento Remoto), Instituto Nacional de Pesquisas Espaciais (INPE), São José dos Campos, 1999. 144 p.
68. SIMOES, S. J. C.; GOMES, L.; MENDES, R. M.; MENDES, T. S. G. SIG e Modelos de escorregamentos: avaliando métodos para reduzir as incertezas de dados de solos e precipitação. RBC. **Revista Brasileira de Cartografia (Online)**, v. 68, p. 1737-1746, 2016.
69. SOETERS, R., VAN WESTEN, C.J. Slope Instability Recognition Analysis and Zonation. In: TURNER, A.K.; SCHUSTER, R.L. (Eds.) **Landslides: Investigation and Mitigation**. National Academy Press, Washington D.C.: 1996, p. 129-177.
70. TATIZANA, C.; OGURA, A.T.; CERRI, L.E.S.; ROCHA, M.C.M. Análise de correlação entre chuvas e escorregamentos na Serra do Mar, município de Cubatão. In: Congresso Brasileiro De Geologia De Engenharia, 1987, São Paulo. **Anais...** São Paulo: ABGE, 1987, p. 225-236.
71. THIEBES, B.; BELL, R.; GLADE, T.; WANG, J.; BAI, S. Application of SINMAP and analysis of model sensitivity - case studies from Germany and China. **Romanian Journal of Geography**, v. 60, n. 1, p. 3-25, 2016.
72. VAN ASCH, T., BUMA, J., VAN BEEK, L.P.H. A view on some hydrological triggering systems in landslides. **Geomorphology**, v. 30, p. 25-32, 1999. Doi: 10.1016/S0169-555X(99)00042-2
73. VAN WESTEN, C.J. Geo-information tools for landslide risk assessment: an overview of recent development. In: LACERDA, M.E; FONTOURA, S.A.B.; SAYAO, A.S.F. (Eds.) **Landslides, Evaluation and Stabilization**. Taylor & Francis Group, Rio de Janeiro: 2004, pp 39-53.
74. VAN WESTEN, C.J.; VAN ASCH, T.W.J.; SOETERS, R. Landslide hazard and risk zonation: why is it still so difficult? **Bulletin of Engineering Geology and Environment**, v. 65, n. 5, p. 167–184, 2006. Doi: 10.1007/s10064-005-0023-0
75. VERA, C.; HIGGINS, W.; AMADOR, J.; AMBRIZZI, T.; GARREAUD, R.; GOCHIS, D.; GUTZLER, D.; LETTENMAIER, D.; MARENGO, J.; MECHOSO, C.R. Toward a Unified View of the American Monsoon Systems. **Climate**, v. 19, p. 4977-5000, 2006. Doi: 10.1175/JCLI3896.1
76. VIEIRA, B.C.; FERREIRA, F.S.G.; VILLAÇA, M.C. Propriedades físicas e hidrológicas dos solos e os escorregamentos rasos na Serra do Mar paulista. **Revista Ra'e Ga - O espaço geográfico em análise**, v. 34, p. 269-287, 2015. Doi: 10.5380/raega.v34i0.40739
77. VIEIRA, B.; GRAMANI, M. Serra do Mar: The Most "Tormented" Relief in Brazil. **World Geomorphological Landscapes**, p. 285-297, 2015. Doi: 10.1007/978-94-017-8023-0_26
78. VIEIRA, B.C.; FERNANDES, N.F.; AUGUSTO FILHO, O.; MARTINS, T.D.; MONTGOMERY, D.R. Assessing shallow landslide hazards using the TRIGRS and SHALSTAB models, Serra do Mar, Brazil. **Environmental Earth Sciences**, v. 77, n. 6, p. 260, 2018. Doi: 10.1007/s12665-018-7436-0
79. WESTRA S, FOWLER HJ, EVANS JP, ALEXANDER LV, BERG P, JOHNSON F, ET AL. Future changes to the intensity and frequency of short-duration extreme rainfall. **Reviews of Geophysics**. 2014;52(3):522-55. Doi: 10.1002/2014RG000464
80. WOLLE, CM. **Análise dos escorregamentos translacionais numa região da Serra do Mar no contexto de uma classificação de mecanismos de instabilização de encosta**. Tese (Doutorado em Engenharia), Universidade de São Paulo, São Paulo, 1988. 500 p.
81. WOLLE, C.M.; CARVALHO, C.S. Deslizamentos em encostas na Serra do Mar - Brasil. **Solos e Rochas**, v. 12, p. 27–36, 1989.

82. WOLLE, C.M.; CARVALHO, C.S. Taludes Naturais. In: FALCONI, F.F.; JUNIOR, A.N. (Org.) **Solos do Litoral de São Paulo**. ABMS, São Paulo: 1994, p. 180-203.
83. WU, W., SIDLE, R.C. A distributed slope stability model for steep forested basins. **Water Resources Research**, v. 31, p. 1097-2110, 1995. Doi: 10.1029/95WR01136
84. WU, Y.; LAN, H.; GAO, X.; LI, L.; YANG, Z. A simplified physically based coupled rainfall threshold model for triggering landslides. **Engineering Geology**, v. 195, p. 63–69, 2015. Doi: 10.1016/j.enggeo.2015.05.022
85. ZIZIOLI, D.; MEISINA, C.; VALENTINO, R.; MONTRASIO, L. Comparison between different approaches to modeling shallow landslide susceptibility: a case history in Oltrepo Pavese, Northern Italy. **Natural Hazards and Earth System Sciences**, v. 13, n. 3, p. 559-73, 2013. Doi: 10.5194/nhess-13-559-2013